Comparison of *Dst* forecast models for intense geomagnetic storms

Eun-Young Ji,[1] Y.-J. Moon,[2] N. Gopalswamy,[3] and D.-H. Lee[2]

Received 24 May 2011; revised 18 January 2012; accepted 22 January 2012; published 10 March 2012.

[1] We have compared six *Dst* forecast models using 63 intense geomagnetic storms ($Dst \leq -100$ nT) that occurred from 1998 to 2006. For comparison, we estimated linear correlation coefficients and RMS errors between the observed *Dst* data and the predicted *Dst* during the geomagnetic storm period as well as the difference of the value of minimum *Dst* ($\Delta Dst_{\min}$) and the difference in the absolute value of *Dst* minimum time (Δt_{Dst}) between the observed and the predicted. As a result, we found that the model by Temerin and Li (2002, 2006) gives the best prediction for all parameters when all 63 events are considered. The model gives the average values: the linear correlation coefficient of 0.94, the RMS error of 14.8 nT, the $\Delta Dst_{\min}$ of 7.7 nT, and the absolute value of Δt_{Dst} of 1.5 hour. For further comparison, we classified the storm events into two groups according to the magnitude of *Dst.* We found that the model of Temerin and Lee (2002, 2006) is better than the other models for the events having $-100 \leq Dst < -200$ nT, and three recent models (the model of Wang et al. (2003), the model of Temerin and Li (2002, 2006), and the model of Boynton et al. (2011b)) are better than the other three models for the events having $Dst \leq -200$ nT.

Citation: Ji, E.-Y., Y.-J. Moon, N. Gopalswamy, and D.-H. Lee (2012), Comparison of *Dst* forecast models for intense geomagnetic storms, *J. Geophys. Res.*, *117*, A03209, doi:10.1029/2011JA016872.

1. Introduction

[2] Geomagnetic storms are large disturbances in the Earth's magnetosphere and are produced by enhanced solar wind-magnetosphere energy coupling through the magnetic reconnection mechanism [*Dungey*, 1961; *Sugiura*, 1964; *Gonzalez et al.*, 1994]. In general, a geomagnetic storm is characterized by a depression in the horizontal (H) component of the geomagnetic field. This depression is mainly caused by the ring current encircling the Earth in a westward direction and can be monitored by the *Dst* index [*Kamide et al.*, 1998; *Daglis et al.*, 1999; *Wang et al.*, 2003]. The *Dst* index is based on measurements from four magnetometers near the equator [*Sugiura and Kamei*, 1991]. It can be calculated by measuring the horizontal geomagnetic field component at four low-latitude ground observatories which represent the effects of several current systems in the low-latitude geomagnetic field [*Akasofu and Chapman*, 1972; *Campbell*, 1996; *Rostoker et al.*, 1997; *Wang et al.*, 2003].

[3] Since the *Dst* is a representative index for indicating a geomagnetic storm, there have been several attempts to forecast it using real-time solar wind data. *Burton et al.* [1975] found that the *Dst* can be well modeled using the solar wind data obtained from spacecraft as input. Their model predicts the ground-based *Dst* index solely from the velocity and density of the solar wind and the B_z component of the interplanetary magnetic field (IMF). Following *Burton et al.* [1975], numerous attempts have been made to improve the *Dst* forecast model [*Murayama*, 1986; *Gonzalez et al.*, 1994, 2004; *Thomsen et al.*, 1998; *Klimas et al.*, 1998; *Fenrich and Luhmann*, 1998; *O'Brien and McPherron*, 2000; *Wang et al.*, 2003; *Temerin and Li*, 2002, 2006; *Xie et al.*, 2008]. Also, the *Dst* index was predicted by neural network methods [*Wu and Lundstedt*, 1996, 1997; *Barkhatov et al.*, 2000; *Lundstedt et al.*, 2002; *Watanabe et al.*, 2003; *Pallocchia et al.*, 2006; *Amata et al.*, 2008] and the NARMAX algorithm [*Boaghe et al.*, 2001; *Boynton et al.*, 2011b]. Some of the above *Dst* forecast models are contributing to the prediction of geomagnetic storms via web pages as a part of the space weather forecast (e.g., http://sprg.ssl.berkeley.edu/dst_index/ and http://lasp.colorado.edu/space_weather/dsttemerin/dsttemerin.html).

[4] The purpose of this study is to compare representative *Dst* forecast models during intense geomagnetic storms ($Dst \leq -100$ nT). For this we consider the following six models as follows: *Burton et al.* [1975], *Fenrich and Luhmann* [1998], *O'Brien and McPherron* [2000], *Wang et al.* [2003], *Temerin and Li* [2002, 2006], and *Boynton et al.* [2011b]. For the input data for the models, we used the solar wind data observed by ACE spacecraft from 1998 to 2006. For a statistical comparison of the *Dst* forecast models, we estimated linear correlation coefficients and RMS (Root Mean Square) errors between the predicted *Dst* data and the observed *Dst* data during geomagnetic storm period. We also obtained the differences between the

[1]Department of Astronomy and Space Science, Kyung Hee University, Yongin, South Korea.
[2]School of Space Research, Kyung Hee University, Yongin, South Korea.
[3]NASA Goddard Space Flight Center, Greenbelt, Maryland, USA.

0148-0227/12/2011JA016872

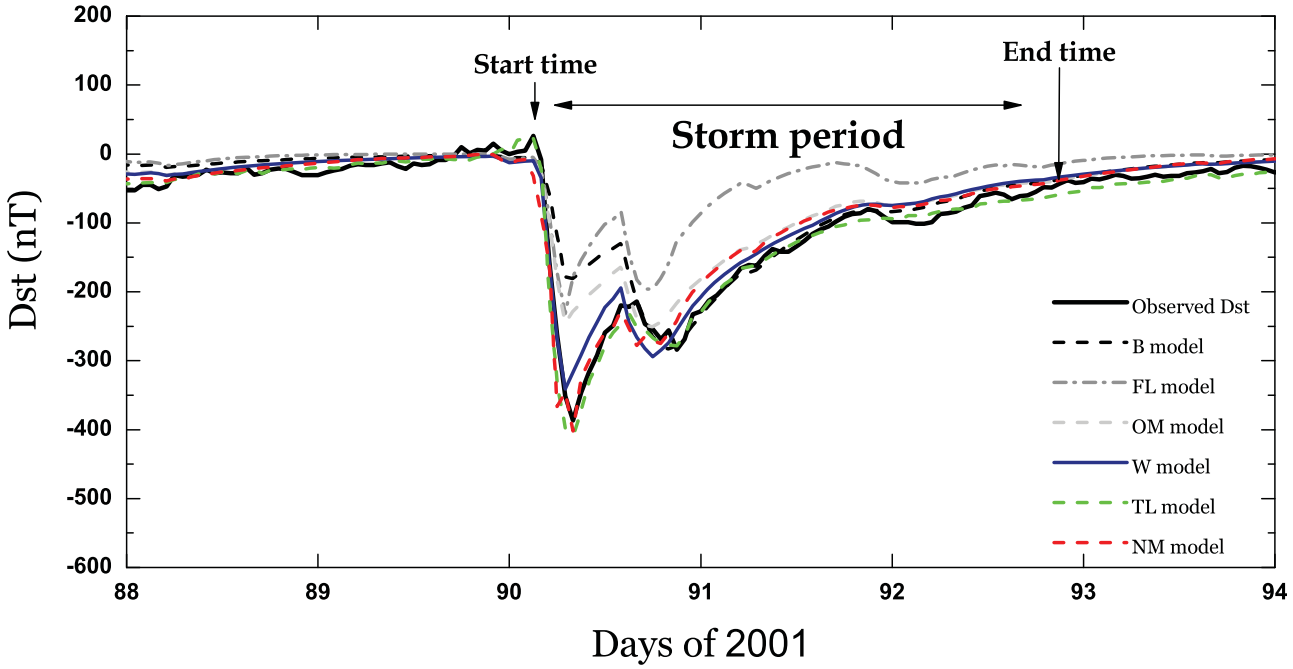

Figure 1. Example of a period of the storm event for the six models.

observed and predicted values of the following quantities: the *Dst* minimum ($\Delta Dst_{\min}$) and the time of the *Dst* minimum (Δt_{Dst}). Also, we classified the intense geomagnetic storm events into four groups depending on the interplanetary structures causing the storms and compared the six *Dst* models for each group. By comparing the statistical models, we identify the best *Dst* forecast model for the prediction of intense geomagnetic storms. The paper is organized as follows. We briefly explain the data and the six *Dst* models in section 2. We present the results of our study in section 3. A brief summary and discussions are given in section 4.

2. Data and Method

2.1. Data

[5] In this study, the observed *Dst* data were obtained from the World Data Center for Geomagnetism, Kyoto (http://wdc.kugi.kyoto-u.ac.jp/). The "Kyoto *Dst*" is calculated every hour and is available in real time from this website. This real time *Dst* values are replaced by provisional values and final values at later dates, which are also available at the Web site. Since the time resolution of observed *Dst* data is an hour, we used the ACE magnetic field and the solar wind data with the same resolution. The ACE spacecraft located in a halo orbit about L1 libration point ~1.5 million km upstream of the Earth. In this study, we considered one hour *Dst* resolution and did not use propagation. The ACE spacecraft data were obtained from the Coordinated Data Analysis Web (CDAWeb) available at NASA's Goddard Space Flight Center (http://cdaweb.gsfc.nasa.gov/cdaweb/). The magnetic field and solar wind velocity vectors are given in the Geocentric Solar Magnetospheric (GSM) coordinate system.

2.2. *Dst* Forecast Models

[6] *Burton et al.* [1975] model (hereinafter referred to as the B model) predicts the *Dst* index based on solar wind data obtained from a spacecraft using the following formula:

$$\frac{dDst^*}{dt} = Q(t) - \frac{Dst^*}{\tau}, \tag{1}$$

where

$$Dst^* = Dst - b\sqrt{P_{dyn}} + c. \tag{2}$$

[7] In the above equations Dst^* is simply the pressure-corrected *Dst*, from which the contribution of the magnetopause current to *Dst* has been eliminated by the equation (2). When the solar wind dynamic pressure is enhanced, the magnetopause moves closer to the Earth, and the currents associated with it contaminate *Dst*. The constant b is a measure of the pressure correction and c is a measure of the quite-time ring current, magnetopause current, and magnetotail current. They determined the constants b and c from the linear regression of ΔDst and $\Delta\sqrt{P}$ (b = 16 nT/(nPa)$^{1/2}$ and c = 20 nT). $Q(t)$ is the rate of ring current injection as a function of the solar wind electric field, $E_y = V_x B_z$, where V_x is an x component of solar wind velocity and B_z is a z component of IMF. τ is a measure of the ring current decay, the value of which corresponds to an e-folding time of 7.7 hours. Several studies have been performed to improve the *Dst* prediction by either modifying Q or τ. *Fenrich and Luhmann* [1998] modified the Burton formula as follows. $Q(t)$ was modified to be dependent of the solar wind dynamic pressure as well as E_y. The value of τ corresponds to an e-folding time of 3 or 5 hours during the main phase of

Table 1. Start Times, End Times, Minimum Value of *Dst*, and Interplanetary Structure of the 63 Storm Events

Number	Start Time (UT)	End Time (UT)	Dst_{min}	Structure[a] (Type)
1	1998/02/17 1200	1998/02/18 1000	−100	nonMC
2	1998/03/10 1100	1998/03/11 1800	−116	CIR
3	1998/05/04 0200	1998/05/05 0200	−205	SH
4	1998/08/26 1000	1998/08/29 0700	−155	nonMC
5	1998/09/25 0100	1998/09/26 0000	−207	SH
6	1998/10/19 0500	1998/10/20 0800	−112	sMC
7	1998/11/09 0300	1998/11/10 1600	−142	sMC
8	1998/11/13 0000	1998/11/15 0400	−131	sMC
9	1999/01/13 1600	1999/01/14 2000	−112	nonMC
10	1999/02/18 0300	1999/02/19 2100	−123	SH
11	1999/09/22 2000	1999/09/23 2300	−173	sMC
12	1999/10/22 0000	1999/10/23 1400	−237	nonMC
13	2000/02/12 0500	2000/02/13 1500	−133	sMC
14	2000/04/06 1700	2000/04/08 0900	−288	SH
15	2000/05/24 0100	2000/05/25 2000	−147	CIR
16	2000/08/10 2000	2000/08/11 1800	−106	nonMC
17	2000/08/12 0200	2000/08/13 1700	−235	sMC
18	2000/10/13 0200	2000/10/14 2300	−107	sMC
19	2000/10/28 2000	2000/10/29 2000	−127	sMC
20	2000/11/06 1300	2000/11/07 1800	−159	sMC
21	2000/11/28 1800	2000/11/29 2300	−119	nonMC
22	2001/03/19 1500	2001/03/21 2300	−149	sMC
23	2001/03/31 0400	2001/04/01 2100	−387	sMC
24	2001/04/11 1600	2001/04/13 0700	−271	sMC
25	2001/04/18 0100	2001/04/18 1300	−114	SH
26	2001/04/22 0200	2001/04/23 1500	−102	sMC
27	2001/08/17 1600	2001/08/18 1600	−105	SH
28	2001/09/30 2300	2001/10/02 0000	−148	nonMC
29	2001/10/21 1700	2001/10/24 1100	−187	SH
30	2001/10/28 0300	2001/10/29 2200	−157	SH
31	2002/03/23 1400	2002/03/25 0500	−100	SH
32	2002/04/17 1100	2002/04/19 0200	−127	sMC
33	2002/04/19 0900	2002/04/21 0600	−149	sMC
34	2002/05/11 1000	2002/05/12 1600	−110	SH
35	2002/05/23 1200	2002/05/24 2300	−109	SH
36	2002/08/01 2300	2002/08/02 0900	−102	SH
37	2002/09/04 0100	2002/09/05 0000	−109	CIR
38	2002/09/07 1400	2002/09/08 2000	−181	SH
39	2002/10/01 0600	2002/10/03 0800	−176	sMC
40	2002/10/03 1000	2002/10/04 1800	−146	sMC
41	2002/11/20 1600	2002/11/22 0600	−128	CIR
42	2003/05/29 2000	2003/05/30 1000	−144	SH
43	2003/06/17 1900	2003/06/19 0300	−141	SH
44	2003/07/11 1500	2003/07/12 1600	−105	CIR
45	2003/08/17 1800	2003/08/19 1100	−148	sMC
46	2003/11/20 1200	2003/11/22 0000	−422	sMC
47	2004/01/22 0300	2004/01/24 0000	−149	nonMC
48	2004/02/11 1000	2004/02/12 0000	−105	CIR
49	2004/04/03 1400	2004/04/04 0800	−112	SH
50	2004/07/22 2000	2004/07/23 2000	−101	nonMC
51	2004/07/24 2100	2004/07/26 1700	−148	sMC
52	2004/07/26 2200	2004/07/30 0500	−197	sMC
53	2004/08/30 0500	2004/08/31 2100	−126	sMC
54	2004/11/07 2100	2004/11/08 2100	−373	sMC
55	2004/11/09 1100	2004/11/11 0900	−289	sMC
56	2004/11/11 2200	2004/11/13 1300	−109	SH
57	2005/01/21 1800	2005/01/23 0500	−105	SH
58	2005/05/07 2000	2005/05/09 1000	−127	CIR
59	2005/05/29 2200	2005/05/31 0800	−138	nonMC
60	2005/06/12 1700	2005/06/13 1900	−106	sMC
61	2005/08/31 1200	2005/09/01 1200	−131	CIR
62	2006/04/13 2000	2006/04/14 2300	−111	sMC
63	2006/12/14 2100	2006/12/16 0300	−147	sMC

[a]Abbreviations are sMC, MC preceded by a fast shock; SH, sheath field; CIR, corotating interaction region; nonMC, ICME that does not show the signature of a magnetic cloud.

the storms when E_y is greater than 4 mV/m and e-folding time 7.7 hours for the remainder of the events. As a result, they found that their model (hereinafter referred to as the FL model) was much better than the B model. Therefore their study implies that during storms the ring current decay is indeed bi-exponential and also that the ring current injection rate increases during periods of enhanced solar wind dynamic pressure. *O'Brien and McPherron* [2000] modified slightly the Burton formula. The constants b and c were determined by a linear fit of the residual phase space offset against $\Delta\sqrt{P}$. A linear fit of the residual phase offset after the removal of Q to the change of the $\sqrt{P}$ yields a pressure correction term b of 7.26 nT/(nPa)$^{1/2}$. And they obtained a value for c of 11 nT. They assumed that the position of ring current is controlled by the E_y during the ring current injection period for southward IMF. Therefore they calculated the Q in terms of E_y (we refer to this model as the OM model). They considered that τ also depend on E_y. The model of *Wang et al.* [2003] (hereinafter referred to as the W model) includes the influences of the solar wind dynamic pressure on Q and τ. His model finds that the strength of Q is proportional to the solar wind dynamic pressure with a power of 0.2 during southward IMF and also that τ is controlled by the size of the magnetosphere for northward IMF. τ decreases as the solar wind dynamic pressure increases, interpreted to be the same as the decrease of the magnetospheric size during the periods of northward IMF. *Wang et al.* [2003] compared their model with the FL model, OM model, and *McPherron and O'Brien* [2001]. They found that the RMS errors for the predicted negative *Dst* obtained using their model are always smaller than those from the other three models. Also, the correlation coefficients between the observed and predicted *Dst* of their model are the highest among the four models. Furthermore they found that the OM model can be substantially improved, especially for intense geomagnetic storms by including the influences of the solar wind dynamic pressure. The model of *Temerin and Li* [2002, 2006] (hereinafter referred to as the TL model) predicts *Dst* by defining differently Q and τ from the other four models. The TL model divides the Q term into three parts (*dst1*, *dst2*, and *dst3*), where each Q term is a function of the current values of the solar wind magnetic field, density, and velocity and of the past values of solar wind magnetic field and of past values of *dst1* and *dst2*. Q terms also have a strong dependence on the angle between the solar wind velocity and Earth's magnetic dipole axis. The τ terms in the three parts have different time constants ranging from 5 days to 1 hour. Temerin and Li compared their model with the B model using data for five years (1995–1999). As a result, they obtained a RMS error of 10.6 nT and a prediction efficiency of 67.6%. Using the original Burton parameters, they obtained a RMS error of 11.8 nT and a prediction efficiency of 59.7%. The model of *Boynton et al.* [2011b] predicts *Dst* differently from the other models. Their model is based on the NARMAX OLS-ERR algorithm that is nonlinear autoregressive moving averages model with exogenous inputs (NARMAX) [*Billings et al.*, 1989; *Boaghe et al.*, 2001; *Balikhin et al.*, 2001] and an orthogonal least squares (OLS) algorithm (hereinafter referred to as the NM model). The NARMAX OLS-ERR algorithm was employed to identify a single input single

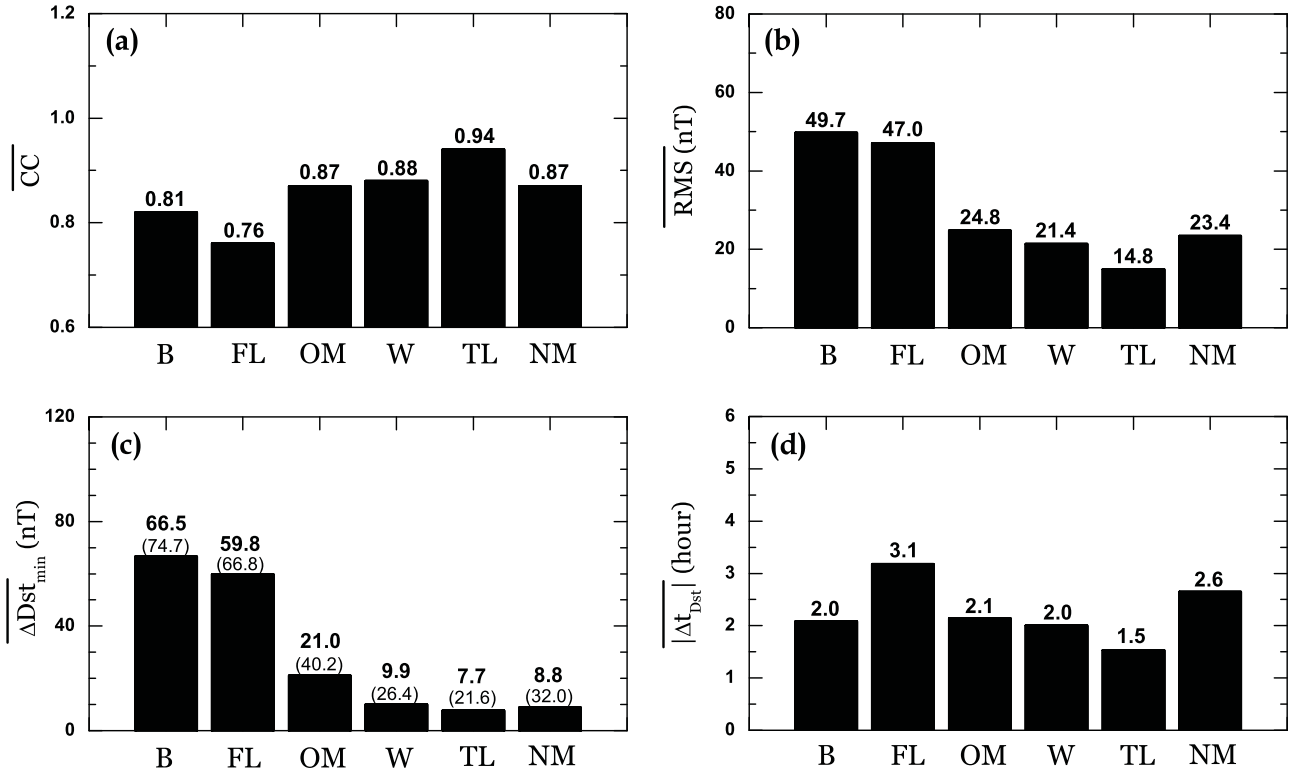

Figure 2. $\overline{CC}$, $\overline{RMS}$, $\overline{\Delta Dst_{\min}}$, and $\overline{|\Delta t_{Dst}|}$ for the six models. The values in parentheses in Figure 2c are the RMS error of $\Delta Dst_{\min}$.

output model (SISO) for predicting the *Dst* using a solar wind-magnetosphere coupling function deduced by *Boynton et al.* [2011a]. They found the best coupling function for the predicting *Dst* model, $C = p^{1/2}V^{4/3}B_T\sin^6(\theta/2)$, where p is the dynamic pressure, V is the solar wind velocity, and θ is the IMF clock angle ($\theta = \tan^{-1}(B_y/B_z)$).

[8] For the input data for the models, we use solar wind data from the ACE spacecraft with 1-hour resolution and obtain the predicted *Dst* with the same resolution. For comparison, the resolution of the predicted value of the TL model was reduced from 5 min to 1 hour by taking the average values. We predicted *Dst* index for 9 years (whole period from 1998 to 2006) with first initial *Dst* value of zero. When run the *Dst* model program for calculating the prediction value of *Dst*, we do not use the observed *Dst* data. We use the only previously predicted *Dst* data.

2.3. Method of Comparison

[9] For comparison we apply the six models to solar wind data during 63 intense geomagnetic storms ($Dst \le -100$ nT) from 1998 to 2006 that were identified by *Zhang et al.* [2007] and *Echer et al.* [2008]. For the quantitative comparisons, we estimated the linear correlation coefficient, the RMS error, the $\Delta Dst_{\min}$, and the Δt_{Dst} of each event for a given model.

[10] First, we determined the start times and the end times of the 63 storm events using the observed *Dst* data. Figure 1 shows the example of period of the storm for the six models. The start times are defined as the times when there were noticeable decrease of *Dst* values after the corresponding interplanetary shocks (Storm Sudden Commencements, SSC) by checking the variation of the solar wind data (velocity, density, and magnetic field). The end times are defined as the times when the *Dst* just recovers to above -50 nT after the minimum *Dst* since we are more interested in lower values of *Dst.* The second and the third columns of Table 1 show the start times and the end times of the 63 storm events.

3. Results

3.1. Statistical Comparison for All Events

[11] We compared statistically the six models by using 63 intense geomagnetic storm events. Figure 2 shows $\overline{CC}$ (correlation coefficient), $\overline{RMS}$, $\overline{\Delta Dst_{\min}}$, and $\overline{|\Delta t_{Dst}|}$ averaged over the 63 storms for the six models. We find that for the all parameters, the TL model is better than the other models. We can also see that the $\overline{\Delta Dst_{\min}}$ values for the W, TL, and NM models are much smaller than those of the other three models in Figure 2c. Figure 3 shows the event number distribution of $\Delta Dst_{\min}$ for the six models. We see that $\Delta Dst_{\min}$ values are positive for most of the storms in the case of the B and FL model that mostly overestimate the *Dst* minimum values. On the other hand, the event number distributions of the W, TL, and NM models are quite symmetric and $\Delta Dst_{\min}$ most of the events are distributed within ± 50 nT. Therefore, the average values for the W, TL, and NM models are small. The RMS errors in $\Delta Dst_{\min}$ (shown in parentheses in Figure 2c) are also smaller for the W, TL, and NM models compared to the other three models.

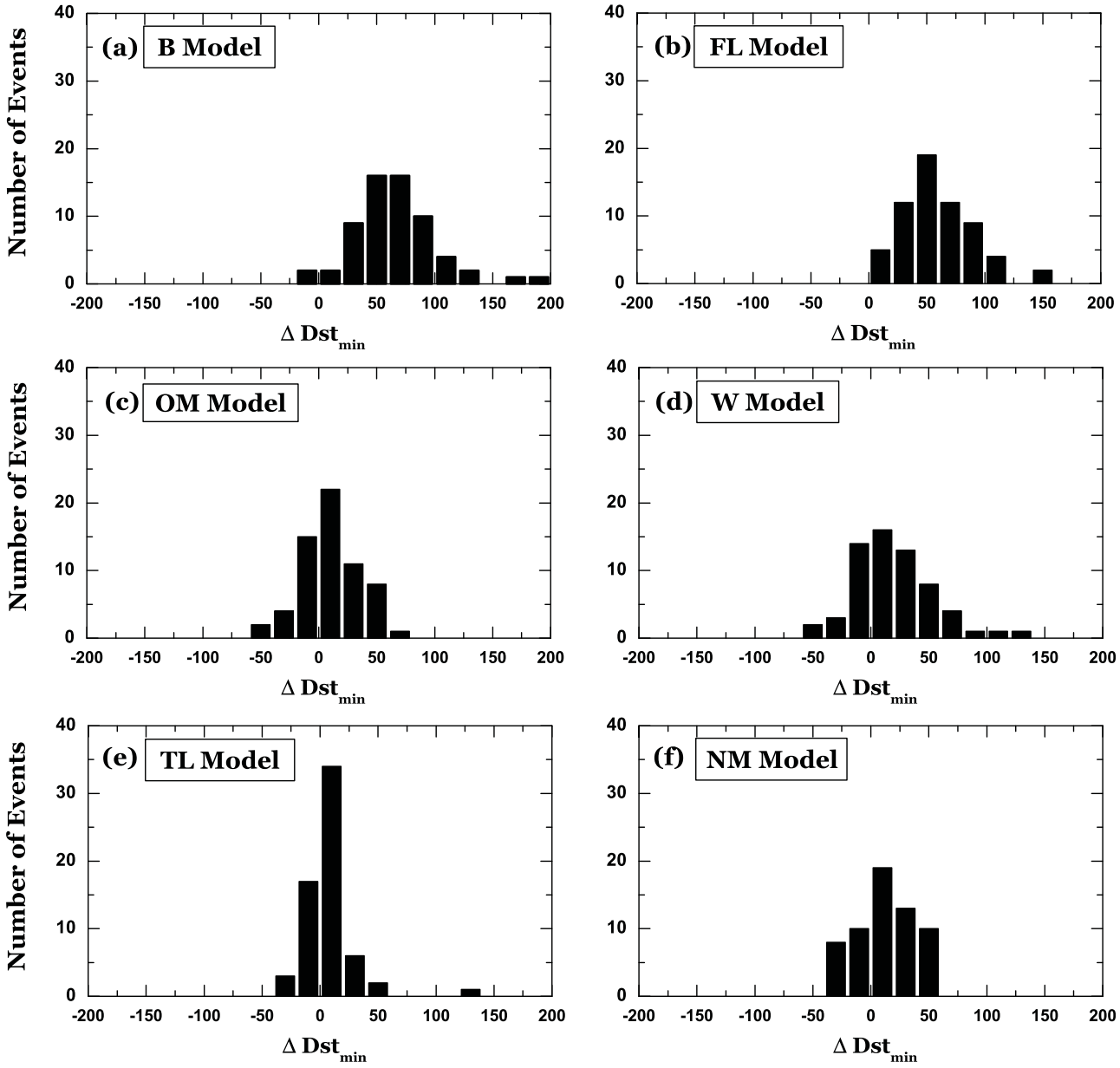

Figure 3. The event number distribution of $\Delta Dst_{\min}$ for the six models: (a) B model, (b) FL model, (c) OM model, (d) W model, (e) TL model, and (f) NM model.

3.2. Dependence on *Dst* Magnitude

[12] For comparison, we classify the storm events into following two groups according to the magnitude of *Dst*: (1) Group 1, 53 storm events having $-100 \le Dst < -200$ nT, and (2) Group 2, 10 super storm events having $Dst \le -200$ nT. The forth column of the Table 1 shows the *Dst* minimum value of events.

[13] Figure 4 shows $\overline{CC}$, $\overline{RMS}$, $\overline{\Delta Dst_{\min}}$, and $\overline{|\Delta t_{Dst}|}$ of the two groups for the six models. We see that $\overline{CC}$ for the TL model is the highest among the six models for the group 1 events, while the $\overline{CC}$ for the W, TL, and NM models are higher compared to the other three models for the group 2 events (see Figure 4a). $\overline{RMS}$ values for the TL model are smaller than those of the other models for both groups (see Figure 4b). The $\overline{\Delta Dst_{\min}}$ for the TL model is the smallest among the six models for the group 1 events, while it is the smallest for the W model for the group 2 events (see Figure 4c). And, the $\overline{\Delta Dst_{\min}}$ value for the NM model is smaller than the other models. Finally, the $\overline{|\Delta t_{Dst}|}$ value for the TL model is the smallest for the group 1 events, while the W model has the smallest value for the group 2 events (see Figure 4d). From these results, we see that the TL model is better than the other models for the storms with $-100 \le Dst < -200$ nT, while the W, TL, and NM models are better than the others for the super storms ($Dst \le -200$ nT).

3.3. Dependence on Interplanetary Structures

[14] In this section, we classified storm events into four groups according to their interplanetary structures causing the storms: 27 sMC events (IP shock and MC), 18 SH events

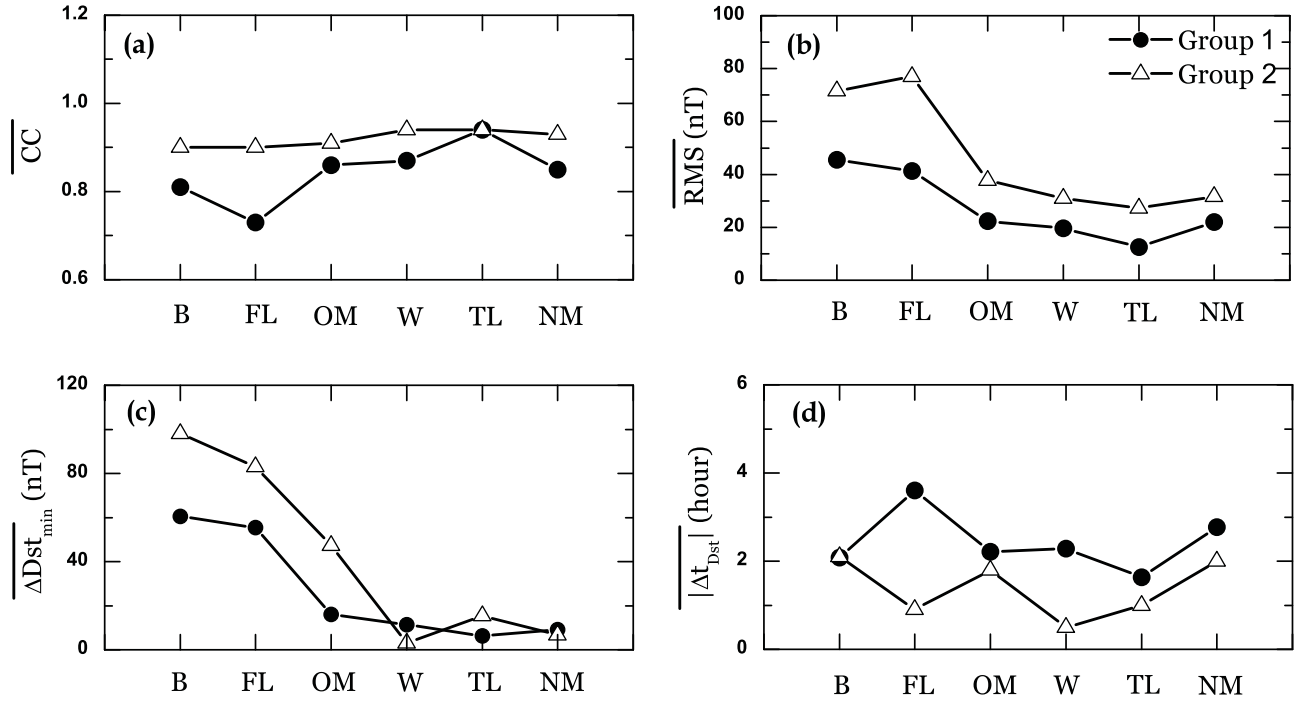

Figure 4. $\overline{CC}$, $\overline{RMS}$, $\overline{\Delta Dst_{\min}}$, and $\overline{|\Delta t_{Dst}|}$ of the two groups for the six models. Group 1 includes the events having $-100 \le Dst < -200$ nT and group 2 includes the events having $Dst \le -200$ nT.

(Sheath Field), 8 CIR events, and 10 nonMC events (non-MC type ICME). The interplanetary structures of these 63 intense geomagnetic storm events were identified by *Echer et al.* [2008]. The fifth column of the Table 1 shows the interplanetary structures of events.

[15] Table 2 shows the $\overline{CC}$ for the four groups. We find that the $\overline{CC}$ values for the TL model are the highest for all groups. Table 3 shows that the $\overline{RMS}$ values for the TL model are the smallest among the six models for all groups. Table 4 shows that the $\overline{\Delta Dst_{\min}}$ values for the TL model are the smallest among the six models except for the SH and the nonMC group. The $\overline{\Delta Dst_{\min}}$ for the NM and the OM models are smallest for the SH group and the nonMC group, respectively. The $\overline{\Delta Dst_{\min}}$ for the TL model are all positive for the non-MC group events; their average value (about 16 nT) of the nonMC group events is higher than those (less than 10 nT) for the other groups. This fact implies that the TL model overestimates *Dst* for this group. Table 5 shows the $\overline{|\Delta t_{Dst}|}$ of the four groups. We find that $\overline{|\Delta t_{Dst}|}$ for the TL model are the smallest among the six models except for the nonMC group. The $\overline{|\Delta t_{Dst}|}$ for the FL model is the smallest for the nonMC group.

4. Summary and Discussions

[16] In this paper, we compared six *Dst* forecast models using 63 intense geomagnetic storms ($Dst \le -100$ nT) that occurred from 1998 to 2006. In particular, we examined the linear correlation coefficient, the RMS error, $\Delta Dst_{\min}$, and Δt_{Dst}. The main results from this study can be summarized as follows.

[17] First, the TL model is better than the other five models when all 63 storms are considered for various parameters. Second, the TL model is better than the other models for storms with $-100 \le Dst < -200$ nT, and the three recent models (the W, TL, and NM models) are better for the super storms ($Dst \le -200$ nT). Third, the TL model is also superior to the other models for all types of interplanetary structures that cause geomagnetic storms. The detailed comparison of these models is summarized in Tables 2–5.

[18] Comparing statistically the six *Dst* forecast models, we conclude that the TL model is best suited for predicting

Table 2. The $\overline{CC}$ of the Four Groups for the Six Models

Model	sMC	SH	CIR	nonMC
B model	0.89	0.71	0.77	0.88
FL model	0.83	0.66	0.66	0.81
OM model	0.9	0.8	0.87	0.9
W model	0.91	0.81	0.87	0.92
TL model	0.94	0.92	0.95	0.94
NM model	0.88	0.82	0.87	0.89

Table 3. The $\overline{RMS}$ (nT) of the Four Groups for the Six Models

Model	sMC	SH	CIR	nonMC
B model	51.4	56.1	48.2	39.2
FL model	51.7	50.0	39.9	34.2
OM model	26.5	27.6	19.0	20.2
W model	22.4	25.4	16.2	15.3
TL model	18.5	12.5	11.8	11.8
NM model	24.1	26.4	19.5	19.6

Table 4. The $\overline{\Delta Dst_{\min}}$ (nT) of the Four Groups for the Six Models

Model	sMC	SH	CIR	nonMC
B model	66.6	68.0	69.7	49.7
FL model	63.2	45.0	53.7	52.0
OM model	20.3	19.2	27.7	4.6
W model	9.6	9.6	16.9	4.8
TL model	5.4	9.0	2.3	15.9
NM model	14.2	1.1	11.7	5.6

intense geomagnetic storms. Temerin and Li considered all the terms used in the B model and tried to add additional solar wind parameters for improvement. The parameters in their model are found by minimizing the RMS error between the predicted *Dst* and the observed *Dst.* In addition, they considered several factors different from the other models as follows. First, the other models calculate the *Dst* by using the pressure-corrected *Dst*, the injection term, and the decay time. The TL model calculates the *Dst* by using the six terms: *dst1*, *dst2*, *dst3*, pressure term, direct IMF B_z term, and offset term. The *dst1*, *dst2*, and *dst3* terms represent three current systems within the magnetosphere: the classic ring current (trapped ions within the dipole-like field of the Earth), the so-called partial ring current, and perhaps the magnetotail current, respectively. The physical interpretation of *dst3* term is not clear. Second, the four other models use only IMF B_z components for determining magetospheric activity. However, the TL model considers the magnitude of the IMF in the $B_z - B_y$ plane. The IMF B_y component also makes an effect on the magnetic reconnection and convection [*Crooker*, 1979; *Gosling et al.*, 1985]. Third, while the TL model takes into account an annual variation and a diurnal variation of *Dst*, other models do not. The annual variation is a function of the angle between the magnetic dipole of the Earth and the solar wind velocity and has both an annual and a diurnal variation [*Cliver et al.*, 2000; *Li et al.*, 2001]. Forth, while the four models use the solar wind electric field E_y component and/or the solar wind dynamic pressure for injection term, the TL model considers the IMF clock angle as well as the IMF B_z component. The four models found the injection functions as $Q \sim VB_s$ and $Q \sim VB_sP$ based on the energy-coupling function between the solar wind and the magnetosphere of *Vasyliunas et al.* [1982]. On the other hand, *Perreault and Akasofu* [1978] and *Akasofu* [1981] considered that the injection into the ring current would occur not only in the southward IMF interval but also for a northward IMF. Thus, Q would depend on the solar wind-magnetosphere energy coupling parameter, $\varepsilon = VB^2\sin^4(\theta/2)$, where B and θ are the strength and the clock angle of the IMF, respectively. However, the TL model showed that there is a strong dependence on the direction of IMF such that magnetic activity depends approximately on the sixth power of the sine of half the IMF clock angle. *Balikhin et al.* [2010] also showed that the coupling functions between solar wind and magnetosphere should be proportional to the sixth power of the sine of half the IMF clock angle and the NM model predicted *Dst* by using such the coupling function.

Table 5. The $\overline{|\Delta t_{Dst}|}$ (hour) of the Four Groups for the Six Models

Model	sMC	SH	CIR	nonMC
B model	1.8	2.0	2.0	2.7
FL model	3.7	2.0	5.1	1.9
OM model	1.8	1.8	2.2	3.2
W model	1.8	1.6	2.3	2.4
TL model	1.5	1.0	1.2	2.3
NM model	3.2	2.1	2.6	2.1

Table 6. $\overline{CC}$, $\overline{RMS}$, $\overline{\Delta Dst_{\min}}$, and $\overline{|\Delta t_{Dst}|}$ Averaged Over the 139 storms (2003–2010) for the Six Models

Parameter	B	FL	OM	W	TL	NM
$\overline{CC}$	0.77	0.75	0.80	0.81	0.88	0.77
$\overline{RMS}$	31.7	25.0	16.7	15.6	15.0	16.9
$\overline{\Delta Dst_{\min}}$	41.4	28.0	5.8	5.2	−3.3	8.1
RMS[a]	46.0	35.4	22.8	19.7	17.4	22.4
$\overline{\lvert\Delta t_{Dst}\rvert}$	2.4	2.7	2.5	2.8	2.1	3.2

[a]The RMS value of $\Delta Dst_{\min}$.

[19] We have examined the error in percentage to find out how well the TL model predicted the *Dst* minimum value. Figure 5 shows the relationship between $\Delta Dst_{\min}/|Dst_{\min}|$ and $|Dst_{\min}|$ for the 63 storm events for the TL model. We find that ∼93% (59/63) of the events are located within ±20%. The RMS error in $\Delta Dst_{\min}/|Dst_{\min}|$ is 0.108. This value means that the error in percentage of the predicted the *Dst* minimum value is ∼11%, which is quite good from the viewpoint of space weather forecast.

[20] In Figure 5, we examined one noticeable outlier event which is the storm that occurred on 20 November, 2003 with an error percentage of 30% (printed by arrow in Figure 5). This event belongs to the group 2 (see section 3.2). All events in the group 2 are located within ±20% except for this storm event. As shown in Figure 4, the average value of $\Delta Dst_{\min}$ for group 2 is 15.3 nT. If we exclude this outlier, the average value becomes 3.2 nT. *Temerin and Li* [2006] explained that because they compared the predicted *Dst* (−300 nT) with the provisional version of the "Kyoto *Dst*" index (−472 nT), this event showed a large difference between them. Although we compared the predicted *Dst* with the final version of the "Kyoto *Dst*" index (−422 nT), this event still shows the largest difference among all events. On the other hand, the W model very well predicts the *Dst* (−420 nT) of this event; its error is only 2 nT. This event is the largest storm of solar cycle 23 and had other peculiarities discussed by *Gopalswamy et al.* [2005].

[21] Temerin and Li found the parameters in the model using by minimizing the RMS error between the predicted *Dst* and observed *Dst* data for eight years (1995–2002). They selected optimized parameters for the model by minimizing the RMS error. Our some events overlap the events of Temerin and Li which are used to decide the parameters in the model. To avoid some arguments on this overlapping, we make another comparison of the six models using 139 storm events ($Dst \leq -50$ nT) from 2003 to 2010. If we consider only intensive storms, the number of data is too small for statistics. We estimated the linear correlation coefficient, the RMS error, $\Delta Dst_{\min}$, and Δt_{Dst}. Table 6 shows $\overline{CC}$, $\overline{RMS}$, $\overline{\Delta Dst_{\min}}$, and $\overline{|\Delta t_{Dst}|}$ averaged over the all storms for the six models. We can see that for the all parameters, the TL model is also better than the other models.

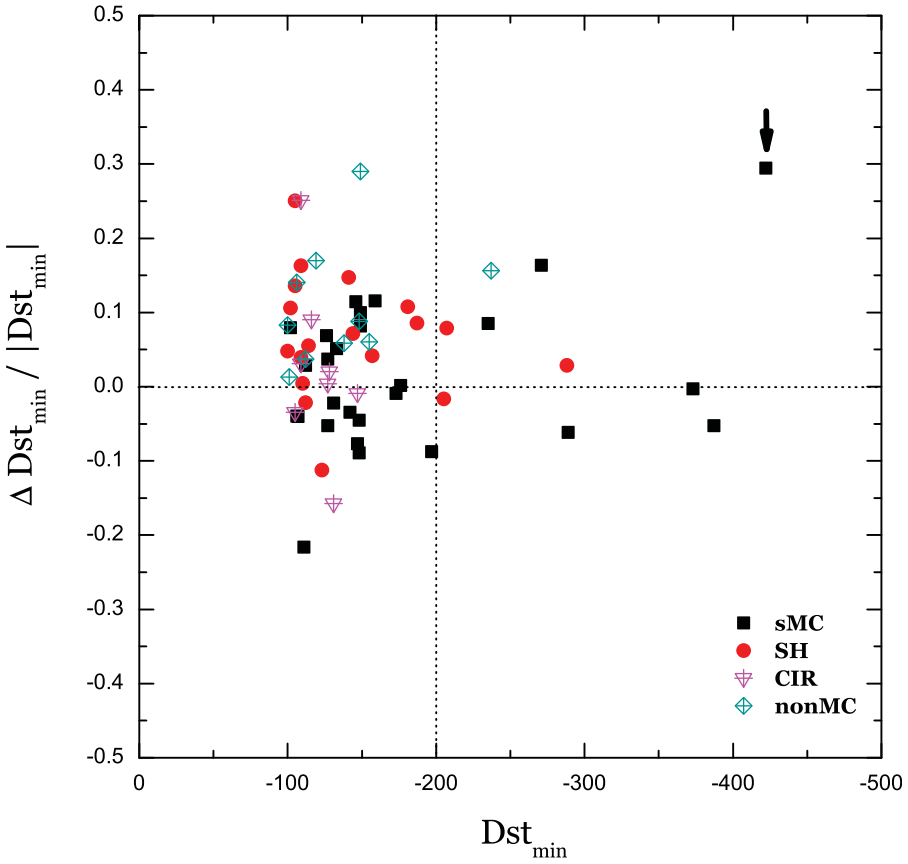

Figure 5. Relationship between $\Delta Dst_{min}/|Dst_{min}|$ and $|Dst_{min}|$ for the TL model. Here the point symbols represent the four interplanetary structures. Super storms ($Dst \leq -200$ nT) are divided by the dotted vertical line.

[22] Relatively, the W, TL, and NM models well predict the super storm events. Among these models,the NM model approach possess advantages over that the W and TL approaches in that NM provides physically interpretable results as demonstrated by *Balikhin et al.* [2010]. Another important point is that the results of the NM model with a modified form of the coupling function allow us to revisit the analytical derivation of this function and pin-point the miscalculation made by *Kan and Lee* [1979].

[23] Our main purpose is to compare the representative *Dst* forecast models for predicting the intense geomagnetic storms and explore suitable models for real-time space weather forecast. We conclude that the TL model is the best *Dst* forecast model for most cases, and the W, TL, and NM models are the best three models for some super storms events. In the near future, we will apply these models to past solar wind data in order to check if these models well predict the occurrence of geomagnetic storms using contingency tables and related statistical parameters [*Ji et al.*, 2010]. Finally, all these results will be used for real-time *Dst* forecast.

[24] **Acknowledgments.** This research was supported by the Kyung Hee University Research Fund (KHU-20101183) in 2010. This work has been also supported by the WCU (World Class University) program through the National Research Foundation of Korea funded by the Ministry of Education, Science and Technology (R31-10016) and by the Korea Research Foundation Grant funded by the Korean Government (MOEHRD, Basic Research Promotion Fund) (KRF-2008-313-C00375, KRF-2008-314-C00158, 20090071744, and 2010-0014501). Y.J.M. is also supported by NASA grant NNX10AL50A. We would like to thank to the WDC-Kyoto for the Dst and the ACE team for the solar wind data.

[25] Philippa Browning thanks the reviewers for their assistance in evaluating this paper.

References

Akasofu, S.-I., (1981), The energy coupling between the solar wind and the magnetosphere, *Space Sci. Rev.*, *28*, 121–190.

Akasofu, S.-I., and S. Chapman (1972), *Solar-Terrestrial Physics*, Oxford Univ. Press, New York.

Amata, E., G. Pallocchia, G. Consolini, M. F. Marcucci, and I. Bertello (2008), Comparison between three algorithms for Dst predictions over the 2003–2005 period, *J. Atmos. Sol. Terr. Phys.*, *70*, 496–502.

Balikhin, M. A., O. M. Boaghe, S. A. Billings, and H. S. C. K. Alleyne (2001), Terrestrial magnetosphere as a nonlinear resonator, *Geophys. Res. Lett.*, *28*, 1123-1126.

Balikhin, M. A., R. J. Boynton, S. A. Billings, M. Gedalin, N. Ganushkina, D. Coca, and H. Wei (2010), Data based quest for solar wind–magnetosphere coupling function, *Geophys. Res. Lett.*, *37*, L24107, doi:10.1029/2010GL045733.

Barkhatov, N. A., N. S. Bellustin, A. E. Leviti, and S. Y. Sakharov (2000), Comparison of efficiency of artificial neural networks for forecasting the geomagnetic activity index Dst, *Radiophys. Quantum Electron.*, *43*, 347–355.

Billings, S. A., S. Chen, and M. J. Korenberg (1989), Identification of MIMO non-linear systems using a forward-regression orthogonal estimator, *Int. J. Control*, *49*, 2157–2189.

Boaghe, O. M., M. A. A. Balikhin, S. A. Billings, and H. Alleyne (2001), Identification of nonlinear processes in the magnetospheric dynamics and forecasting of Dst index, *J. Geophys. Res.*, *106*, 30,047–30,066.

Boynton, R. J., M. A. Balikhin, S. A. Billings, H. L. Wei, and N. Ganushkina (2011a), Using the NARMAX OLS-ERR algorithm to obtain the most influential coupling functions that affect the evolution of the magnetosphere, *J. Geophys. Res.*, *116*, A05218, doi:10.1029/2010JA015505.

Boynton, R. J., M. A. Balikhin, S. A. Billings, A. S. Sharma, and O. A. Amariutei (2011b), Data derived NARMAX Dst model, *Ann. Geophys.*, *29*, 965–971.

Burton, R. K., R. L. McPherron, and C. T. Russell (1975), An empirical relationship between interplanetary conditions and Dst, *J. Geophys. Res.*, *80*, 4204–4214.

Campbell, W. H. (1996), Geomagnetic storms, the Dst ring-current myth and lognormal distributions, *J. Atmos. Sol. Terr. Phys.*, *58*, 1171–1187.

Cliver, E. W., Y. Kamide, and A. G. Ling (2000), Mountains versus valleys: Semiannual variation of geomagnetic activity, *J. Geophys. Res.*, *105*, 2413–2424.

Crooker, N. U. (1979), Dayside merging and cusp geometry, *J. Geophys. Res.*, *84*, 951–959.

Daglis, I. A., R. M. Thorne, W. Baumjohann, and S. Orsini (1999), The terrestrial ring current: Origin, formation, and decay, *Rev. Geophys.*, *37*, 407–438.

Dungey, J. W. (1961), Interplanetary magnetic field and the auroral zones, *Phys. Rev. Lett.*, *6*, 47–48.

Echer, E., W. D. Gonzalez, B. T. Tsurutani, and A. L. C. Gonzalez (2008), Interplanetary conditions causing intense geomagnetic storms ($Dst \leq -100$ nT) during solar cycle 23 (1996–2006), *J. Geophys. Res.*, *113*, A05221, doi:10.1029/2007JA012744.

Fenrich, F. R., and J. G. Luhmann (1998), Geomagnetic response to magnetic clouds of different polarity, *Geophys. Res. Lett.*, *25*, 2999–3002.

Gonzalez, W. D., J. A. Joselyn, Y. Kamide, H. W. Kroehl, G. Rostoker, B. T. Tsurutani, and V. M. Vasyliunas (1994), What is a geomagnetic storm?, *J. Geophys. Res.*, *99*, 5771–5792.

Gonzalez, W. D., A. Dal Lago, A. L. Clúa de Gonzalez, L. E. A. Vieira, and B. T. Tsurutani (2004), Prediction of peak-Dst from halo CME/magnetic cloud-speed observations, *J. Atmos. Sol. Terr. Phys.*, *66*, 161–165.

Gopalswamy, N., S. Yashiro, G. Michalek, H. Xie, R. P. Lepping, and R. A. Howard (2005), Solar source of the largest geomagnetic storm of cycle 23, *Geophys. Res. Lett.*, *32*, L12S09, doi:10.1029/2004GL021639.

Gosling, J. T., D. N. Baker, S. J. Bame, W. C. Feldman, and E. J. Smith (1985), North-south and dawn-dusk plasma asymmetries in the distant tail lobes: ISEE 3, *J. Geophys. Res.*, *90*, 6354–6360.

Ji, E.-Y., Y.-J. Moon, K.-H. Kim, and D.-H. Lee (2010), Statistical comparison of interplanetary conditions causing intense geomagnetic storms ($Dst \leq -100$ nT), *J. Geophys. Res.*, *115*, A10232, doi:10.1029/2009JA015112.

Kamide, Y., et al. (1998), Current understanding of magnetic storms: Storm-substorm relationships, *J. Geophys. Res.*, *103*, 17,705–17,728.

Kan, J. R., and L. C. Lee (1979), Energy coupling function and solar wind–magnetosphere dynamo, *Geophys. Res. Lett.*, *6*, 577–580.

Klimas, A. J., D. Vassiliadis, and D. N. Baker (1998), *Dst* index prediction using data-derived analogues of the magnetospheric dynamics, *J. Geophys. Res.*, *103*, 20,435–20,447.

Li, X., D. N. Baker, S. G. Kanekal, M. Looper, and M. Temerin (2001), Long-term measurements of radiation belts by SAMPEX and their variations, *Geophys. Res. Lett.*, *28*, 3827–3830.

Lundstedt, H., H. Gleisner, and P. Wintoft (2002), Operational forecasts of the geomagnetic *Dst* index, *Geophys. Res. Lett.*, *29*(24), 2181, doi:10.1029/2002GL016151.

McPherron, R. L., and T. P. O'Brien (2001), Prediction geomagnetic activity: The Dst index, in *Space Weather*, *Geophys. Monogr. Ser.*, vol. 125, edited by P. Song, H. J. Singer, and G. L. Siscoe, pp. 339–345, AGU, Washington, D. C.

Murayama, T. (1986), Coupling function between the solar wind and the Dst index, in *Solar Wind–Magnetosphere Coupling*, edited by Y. Kamide and J. A. Slavin, p. 119, Terra Sci., Tokyo.

O'Brien, T. P., and R. L. McPherron (2000), An empirical phase space analysis of ring current dynamics: Solar wind control of injection and decay, *J. Geophys. Res.*, *105*, 7707–7720.

Pallocchia, G., E. Amata, G. Consolini, M. F. Marcucci, and I. Bertello (2006), Geomagnetic Dst index forecast based on IMF data only, *Ann. Geophys.*, *24*, 989–999.

Perreault, P., and S.-I. Akasofu (1978), A study of geomagnetic storms, *Geophys. J. R. Astron. Soc.*, *54*, 547–551.

Rostoker, G., E. Friedrich, and M. Dobbs (1997), Physics of magnetic storms, in *Magnetic Storms*, *Geophys. Monogr. Ser.*, vol. 98, edited by B. T. Tsurutani et al., pp. 149–160, AGU, Washington, D. C.

Sugiura, M. (1964), Hourly values of equatorial Dst for the IGY, in *Annual International Geophysical Year*, vol. 3, p. 9, Pergamon, New York.

Sugiura, M., and T. Kamei (1991), Equatorial Dst index 1957–1986, *IAGA Bull., 40*, Publ. Off., Int. Serv. Geomagn. Indices, Saint-Maur-des-Fosses, France.

Temerin, M., and X. Li (2002), A new model for the prediction of *Dst* on the basis of the solar wind, *J. Geophys. Res.*, *107*(A12), 1472, doi:10.1029/2001JA007532.

Temerin, M., and X. Li (2006), *Dst* model for 1995–2002, *J. Geophys. Res.*, *111*, A04221, doi:10.1029/2005JA011257.

Thomsen, M. F., J. E. Borovsky, D. J. McComas, and M. R. Collier (1998), Variability of the ring current source population, *Geophys. Res. Lett.*, *25*, 3481–3484.

Vasyliunas, V. M., J. R. Kan, G. L. Siscoe, and S.-I. Akasofu (1982), Scaling relations governing magnetospheric energy transfer, *Planet. Space Sci.*, *30*, 359–365.

Wang, C. B., J. K. Chao, and C. H. Lin (2003), Influence of the solar wind dynamic pressure on the decay and injection of the ring current, *J. Geophys. Res.*, *108*(A9), 1341, doi:10.1029/2003JA009851.

Watanabe, S., E. Sagawa, K. Ohtaka, and H. Shimazu (2003), Operational models for forecasting Dst, *Adv. Space Res.*, *31*, 829–834.

Wu, J.-G., and H. Lundstedt (1996), Prediction of geomagnetic storms from solar wind data using Elman recurrent neural networks, *Geophys. Res. Lett.*, *23*, 319–322.

Wu, J.-G., and H. Lundstedt (1997), Neural network modeling of solar wind–magnetosphere interaction, *J. Geophys. Res.*, *102*(A7), 14,457–14,466.

Xie, H., N. Gopalswamy, O. C. St. Cyr, and S. Yashiro (2008), Effects of solar wind dynamic pressure and preconditioning on large geomagnetic storms, *Geophys. Res. Lett.*, *35*, L06S08, doi:10.1029/2007GL032298.

Zhang, J., et al. (2007), Solar and interplanetary sources of major geomagnetic storms ($Dst \leq -100$ nT) during 1996–2005, *J. Geophys. Res.*, *112*, A10102, doi:10.1029/2007JA012321.

N. Gopalswamy, NASA Goddard Space Flight Center, Greenbelt, MD 20771, USA. (gopals@fugee.gsfc.nasa.gov)

E.-Y. Ji, Department of Astronomy and Space Science, Kyung Hee University, Yongin 446-701, South Korea. (eyji@khu.ac.kr)

D.-H. Lee and Y.-J. Moon, School of Space Research, Kyung Hee University, Yongin 446-701, South Korea. (dhlee@khu.ac.kr; moonyj@khu.ac.kr)